THE JOURNAL OF PHYSICAL CHEMISTRY B

ARTICLE

pubs.acs.org/JPCB

Structure of Colloidal Solution in Presence of Mixed Electrolytes: A Solvent Restricted Primitive Model Study

Brindaban Modak, Chandra N. Patra,*,† Swapan K. Ghosh, and Priyanka Das

Theoretical Chemistry Section, Chemistry Group, Bhabha Atomic Research Centre, Mumbai 400 085, India

ABSTRACT: The structure of colloidal solution in presence of mixed electrolytes is studied using Monte Carlo simulation and density functional theory, based on a four-component model of the spherical double layer. In this model the ions and solvent molecules are treated as charged and neutral hard spheres, respectively, having equal diameter, and in addition the mixture of mono- and multivalent co-ions are also considered. The macroion is considered as a uniformly charged hard sphere surrounded by the electrolyte and the solvent. The density functional theory is based on a partially perturbative scheme, where the electrical part is calculated through perturbation with respect to uniform density and the hard sphere contribution is approximated using a weighted density approach. The theory is found to be in quantitative agreement with the Monte Carlo simulation results, for singlet density as well as the mean electrostatic potential profiles. The system is studied over a wide range of parametric conditions, viz. with different ionic valences as well as size, at varying electrolyte concentration ratio of mono- and multivalent co-ions of mixed electrolytes, at different surface charge densities, and radius of the macroion. The present work reflects that even a simple primitive model for the solvent is able to manipulate the hard-sphere and electrostatic correlations of the diffuse double layer in the ionic density as well as mean electrostatic potential profiles.

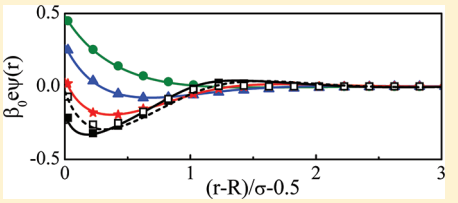

I. INTRODUCTION

When a charged surface is immersed in an electrolyte solution, it is surrounded by smaller counterions and co-ions resulting in a uniform neutralizing background. The local perturbation resulting into separation of charge in the electrode−electrolyte interface is commonly called as electric double layer (EDL).[1,2] The formation of EDL is quite significant in many interfacial phenomena relating to physical chemistry.[3,4] For instance, the stability of colloidal dispersions and their coagulation properties are directly influenced by the properties of the EDL formed.[5] Electrochemical reactions mostly occur at interfaces, hence the kinetics of these reactions will be largely dependent on ionic distributions.[6] The mean electrostatic potential (MEP) around the macroion is a quantity of central importance in colloid science, that determines the flocculation or the migration of macroparticles in a colloidal system. The MEP is usually identified with the well-known electrokinetic potential at the slipping plane (i.e., zeta potential) as a function of distance from the macroion surface. The zeta potential is an experimentally determined quantity, which displays various electrokinetic effects[7] such as electrophoresis, electro-osmosis, and streaming currents, and is quite useful in the characterization, separation, and manufacture of colloidal substances. Distribution of small ions in EDLs is largely dependent on salt characteristics that directly or indirectly affect the behavior of DNA and several other biomacromolecules.[8] Hence, a systematic study of microscopic structure of EDL is necessary to understand the effect of various parameters on its properties.

Depending on the charged surface, EDL exists in different geometries[9] such as planar,[10−13] cylindrical,[14−18] spherical,[19−24] and ellipsoidal.[25,26] Over the decades, several research groups have focused their attention on investigating the properties of EDL in different geometries for the interpretation of various experimental findings. However, systematic theoretical investigation of the spherical double layer (SDL) is far from being complete and got a new look only recently.[27] For proper explanation of phenomena involving colloidal solutions,[2] the spherical double layer (SDL) model is supposed to be the best suited one.[28] Examples for electric double layers of spherical symmetry include polyelectrolyte solutions, micelles, synapses, phospholipid vesicles, and microemulsions.[29,30] Polyelectrolytes[31] are large charged groups, which usually form spherical conformations to minimize the electrostatic repulsions. Micelles are small aggregates of amphiphilic molecules in aqueous solutions, while microemulsions are produced in the mixtures of water and oil in presence of ampliphilic molecules, which separates into different domains of water in oil (or oil in water). SDL is sufficiently simple and convenient model to represent such multiparticle systems and systems of more complex composition. Several tailored macromolecules having polymeric and oligomeric tethers can also be studied by utilizing simple and convenient model of SDL.[32] The structure of SDL provides the microscopic description of the electrostatic mobility of charged colloidal particles including globular proteins.

It is now quite well established that phenomenon like ionic layering, charge inversion, and overcharging are usually associated

Received: May 26, 2011
Revised: September 14, 2011
Published: September 15, 2011

dx.doi.org/10.1021/jp204913d | J. Phys. Chem. B 2011, 115, 12126–12134

with multivalent electrolytes in concentrated solutions.[19,33,34] Briefly, the oscillating ionic distribution near the electrode surface is referred to as layering.[21] The phenomena of crossing of co-ion density to that of counterions due to stronger electrostatic attraction of macroion with the counterions is known as charge inversion. Overcharging refers to the increase of macroion charge due to unusual adsorption of co-ions.[34] Mixed electrolytes containing multivalent ions are also quite important in biophysics.[35] Hence, investigation of the property of SDLs in presence of different mixed electrolyte solutions containing multivalent ions is a fascinating issue to determine the relevance of ion correlations in the electrolyte mixtures as well as to improve the knowledge about the phenomena related to the structure and dynamics of macromolecular solutions.

This last decade has seen a continuous emergence of several sophisticated models to describe EDL theoretically leading to significant advances in this field. The most widely used simple model to describe the double layer structure is the restricted primitive model (RPM),[1] where the ions are represented by charged hard spheres, immersed in a uniform, isotropic dielectric continuum medium. Here, the "colloid" particle is mimicked as a uniformly charged hard sphere. Although, in this model, the solvent structure near the charged surface remains uniform, the ionic distribution including the experimental capacitance data can be obtained quite quantitatively. However, in many cases, the solvent plays an important role; hence, RPM fails to explain many electrokinetic properties related to colloidal suspensions. A complete molecular description of the electrolyte solution requires treating the ions as well as the solvent molecules as explicit components. In the molecular solvent model (MSM) the ions and solvent molecules are treated as charged and neutral hard spheres of finite size, respectively. In this approach, the solvent molecule is considered as highly polar molecules with permanent dipoles, quadrupoles, etc. However, the implementation of MSM is computationally very expensive as it includes the ion−solvent and solvent−solvent interactions explicitly along with the ion−ion interactions. In the present study we consider a relatively simpler approach, known as solvent restricted primitive model (SRPM).[36,37] In the SRPM, the solvent molecules of an electrolyte are explicitly represented as hard spheres, whereas the electrostatic contribution of the solvent is expressed implicitly by a uniform dielectric medium in which charged hard sphere ions interact; that is, the steric effect of the solvent molecule is considered, whereas the solvent polarization is completely neglected. In contrast to RPM, the present model can represent the molecular packing more realistically. However, consideration of all-atom models with explicit water and ions through simulations may serve as a better description of SDL.[38]

Simulations generally provides realistic description of model systems, hence are used regularly to test the accuracy of different theoretical predictions. The first simple model of SDL was treated by classical Poisson−Boltzmann (PB) theory, which is based on a point-charge representation of the electrolyte in a dielectric continuum.[28,39] The results from the PB theory are found to be in good agreement with the results of Monte Carlo (MC) simulation in case of monovalent electrolytes at moderate concentrations. The PB formalism breaks down when the crowding of ions becomes significant, i.e., correlations between particles become potentially important. For systems with multivalent counterions and co-ions at high salt concentration, PB formalism cannot describe the phenomena of the oscillatory behavior of the ionic concentration profiles as well as charge reversal. Incorporation of the electrostatic correlations and the ionic exclusion volume effects give rise to the modified Poisson−Boltzmann (MPB) theory,[40] which shows a better agreement with the MC simulations to describe equilibrium ion profiles near a charged surface. Integral equation theory (IET) with correlations included through the hypernetted chain/mean spherical approximation (HNC/MSA) also provide concentration profiles quite accurately.[19,20]

With the convergence of all theoretical approaches to include correlations of small ions quite effectively, density functional theory (DFT) appears to be a powerful tool for quantitative prediction of structural and associated thermodynamic properties of SDL when compared with the Monte Carlo simulation results.[23,24,27] According to classical DFT, the grand potential should be expressible in terms of singlet density, which attains a minimum value at the true equilibrium density.[41] The exact form of the grand potential functional for the nonuniform system is usually not known in general, hence to be approximated with known structural quantities of the corresponding uniform systems. This approximate route resulted to the development of several perturbative and nonperturbative methods as applied to SDL.

In this work, we present a detailed investigation of the structure of SDL in presence of a mixed electrolyte in the framework of the solvent restricted primitive model (SRPM) using DFT and MC simulation. The hard sphere interaction is calculated using a weighted density approximation (WDA) based on the Denton and Ashcroft recipe,[42] whereas the residual Coulombic contribution is approximated through perturbation with respect to the bulk ionic fluid. The finite size of the solvent molecules has been taken into account in the canonical ensemble MC simulations performed here. Present study shows that the density profiles for the small ions and the solvent molecules as well as the mean electrostatic potential profiles predicted from the DFT matches well with that obtained from the simulation under various macroscopic condition, such as at different ionic valences as well as size, at varying electrolyte concentration ratios of mono- and multivalent co-ions of mixed electrolytes, at different surface charge densities and radius of the macroion. The excluded volume effects due to the presence of solvent molecules as an individual component have been reflected in the density as well as potential profiles of all the systems studied here. The remainder of this paper is organized as follows. The computational method including the respective model and the theoretical formalism are discussed in section II, the numerical results are presented in section III, and some concluding remarks are given in section IV.

II. THEORETICAL FORMULATION

A. Solvent Restricted Primitive Model. The model involved in the present study, considers the molecular nature of the solvent molecules as an external component in addition to the mixture of mono- and multivalent co-ions. The spherical double layer (SDL) model utilized here consists of an isolated, rigid, and impenetrable spherical colloid of radius R having a uniform surface charge density Q given as

$$Q = \frac{Ze}{4\pi R^2} \tag{1}$$

where Z is the valence of the macroparticle and e is the electronic charge. The macroion is immersed in a mixed 1:2:1 $NaCl/MgCl_2$

electrolyte solution. The electrolyte solution consists of small ions ($\alpha = 1-3$), which are treated as hard sphere of equal diameter σ with embedded point charges of valences z_α at their centers. In essence, the system consists of four components, $\alpha = 1-4$, where the fourth component represents the solvent ($z_\alpha = 0$ for $\alpha = 4$). Apart from its molecular nature, the solvent is also considered as a uniform dielectric continuum with the dielectric constant taken as that of water, $\varepsilon = 78.5$ at temperature $T = 298$ K. In all cases of SRPM, the concentration of the solvent is kept fixed at 8.65 M unless otherwise mentioned, which is equivalent to reduced bulk density of the solvent as $\rho_4^{0*}[= \rho_4^0\sigma^3] = 0.4$ for hard sphere size of 4.25 Å. The concentration of the solvent is kept so low instead of around 55.5 M, which is the bulk water solvent concentration, mainly because of the difficulty associated with accommodating a large number of molecules in a simulation box of finite dimensions and its efficient sampling. Thus it was a compromise to take the solvent in the moderate concentrations so as to do the simulations efficiently and also to incorporate sufficient steric interactions.

The interaction potential between the macroion and small ion is given as

$$U_{M\alpha}(r) = \begin{cases} \dfrac{4\pi R^2 Q z_\alpha e}{\varepsilon r_\alpha}, & r_\alpha \geq R + \dfrac{\sigma}{2} \\ \infty, & \text{otherwise} \end{cases} \quad (2)$$

where z_α is the valence of ion α and r_α is its radial distance from the macroion surface. The interaction potential between two small ions is given by

$$U_{\alpha\beta}(r) = \begin{cases} \dfrac{z_\alpha z_\beta e^2}{\varepsilon r}, & r \geq \sigma \\ \infty, & \text{otherwise} \end{cases} \quad (3)$$

with r as the interionic distance. The typical value for the diameter of the small ions is considered as $\sigma = 4.25$ Å, except for the cases where there is a variation of size of the small ion. The hard-core interaction potential at contact between the polyion and the small ions and also among all (charged and neutral) hard spheres can be recovered by putting $z_\alpha = 0$ in eqs 3 and 2.

B. Density Functional Theory. In classical DFT, the grand potential Ω for the system consisting of small ions surrounding an isolated charged macroparticle is related to the Helmholtz free energy functional F through the Legendre transform

$$\Omega[\{\rho_\alpha\}] = F[\{\rho_\alpha\}] + \sum_\alpha \int d\mathbf{r}\, \rho_\alpha(\mathbf{r})[U_{M\alpha}(\mathbf{r}) - \mu_\alpha] \quad (4)$$

where $\{\rho_\alpha\}$ is a set of density distributions for all of the components including the solvent and μ_α is the chemical potential of component α. Utilizing the fact that the grand potential $\Omega[\{\rho_\alpha\}]$ attains a minimum value at equilibrium, the final expression for the component ionic density distribution $\rho_\alpha(\mathbf{r})$ in the field of the colloidal macroion and in equilibrium with the bulk phase of density ρ_α^0 is given by

$$\rho_\alpha(r) = \rho_\alpha^0 \exp\{-\beta_0 z_\alpha \psi(r) + c_\alpha^{(1)\mathrm{hs}}(r;[\{\rho_\alpha\}]) - c_\alpha^{(1)\mathrm{hs}}([\{\rho_\alpha^0\}]) + c_\alpha^{(1)\mathrm{el}}(r;[\{\rho_\alpha\}]) - c_\alpha^{(1)\mathrm{el}}([\{\rho_\alpha^0\}])\} \quad (5)$$

where $\psi(r)$ corresponds to the MEP of the SDL system that arises due to interaction between the macroion surface charge and the small ion distribution and can be expressed as

$$\psi(r) = \frac{4\pi e}{\epsilon}\int_r^\infty \sum_\alpha z_\alpha \rho_\alpha(r')\left(r' - \frac{r'^2}{r}\right) dr' \quad (6)$$

Here, $c_\alpha^{(1)\mathrm{hs}}(r;[\{\rho_\alpha\}])$ and $c_\alpha^{(1)\mathrm{el}}(r;[\{\rho_\alpha\}])$ stand for first order correlation function component from the hard-sphere and the electrical contributions, respectively. In spite of the exact nature of eq 5, it cannot be solved due to inadequacy of explicit forms of $c_\alpha^{(1)\mathrm{hs}}$ and $c_\alpha^{(1)\mathrm{el}}$ for the nonuniform SDL. Hence, a weighted density approximation (WDA) of Denton and Ashcroft (DA),[42] is employed as

$$c_\alpha^{(1)\mathrm{hs}}(\mathbf{r};[\{\rho_\alpha\}]) = \tilde{c}_\alpha^{(1)\mathrm{hs}}(\overline{\rho}^{(\alpha)}(\mathbf{r})) \quad (7)$$

where the effective density $^{(\alpha)}(r)$ is defined as

$$\overline{\rho}^{(\alpha)}(\mathbf{r}) = \sum_\beta \int d\mathbf{r}'\, \rho_\beta(\mathbf{r}') w_{\alpha\beta}^{\mathrm{hs}}(|\mathbf{r}-\mathbf{r}'|;\overline{\rho}^{(\alpha)}(\mathbf{r})) \quad (8)$$

and $w_{\alpha\beta}^{\mathrm{hs}}(r)$ is the weight function obtained from the DA recipe[42]

$$w_{\alpha\beta}^{\mathrm{hs}}(\mathbf{r};\overline{\rho}^{(\alpha)}(\mathbf{r})) = \frac{\tilde{c}_{\alpha\beta}^{(2)\mathrm{hs}}(\mathbf{r};\overline{\rho}^{(\alpha)}(\mathbf{r}))}{\partial\tilde{c}_\alpha^{(1)\mathrm{hs}}/\partial\rho|_{\overline{\rho}^{(\alpha)}(\mathbf{r})}} \quad (9)$$

The electrical contribution, however, has been evaluated as a perturbation around the uniform fluid as

$$c_\alpha^{(1)\mathrm{el}}(\mathbf{r};[\{\rho_\alpha\}]) - c_\alpha^{(1)\mathrm{el}}([\{\rho_\alpha^0\}]) = \sum_{\beta=1}^{2}\int d\mathbf{r}'\tilde{c}_{\alpha\beta}^{(2)\mathrm{el}}(|\mathbf{r}-\mathbf{r}'|;\{\rho_\alpha^0\})[\rho_\beta(\mathbf{r}') - \rho_\beta^0] \quad (10)$$

The analytical expression for $\tilde{c}_{\alpha\beta}^{(2)\mathrm{el}}$ is used from the mean spherical approximation (MSA)[43] and is given as

$$\tilde{c}_{\alpha\beta}^{(2)el}(\mathbf{r};[\{\rho_\alpha^0\}]) = -\frac{\beta_0 z_\alpha z_\beta e^2}{\varepsilon}\left[\frac{2B}{\sigma} - \left(\frac{B}{\sigma}\right)^2 \mathbf{r} - \frac{1}{\mathbf{r}}\right] \quad (11)$$

for $r < \sigma$ and 0 otherwise, with the coefficient B has its usual meaning. The density profiles for the small ions and the solvent molecules in a SDL can be calculated using eq 5 through a self-consistent iterative procedure.

C. Monte Carlo Simulation. In the present study, we perform a canonical ensemble (NVT) Monte Carlo simulation using a standard Metropolis sampling procedure.[44] A cubic simulation cell with the macroion fixed at its center and surrounded by the small ions and solvent molecules is adopted here. The usual periodic boundary conditions are employed in all directions and sufficiently large box has been taken to avoid macroion-macroion interactions. To maintain elctroneutrality, the number of ions for each species (N_α) is adjusted according to the relation: $\Sigma_\alpha N_\alpha z_\alpha + Ze = 0$.

During each simulation cycle, one of the components (small ion or the solvent) is arbitrarily chosen inside the simulation cell and allowed to move through a small random distance. The total potential energy of the system decides the selection criteria for any move. The move is restricted in such a way that after every move, there should not be any overlap between the small ion and the macroion and also within the small ions. Owing to small plasma parameter ($\Gamma < 10$) and large simulation box, the Ewald

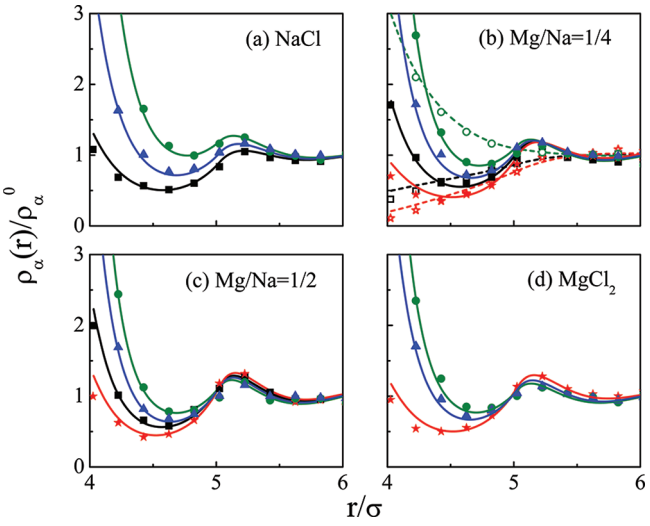

Figure 1. Small ion density profiles around a spherical macroion of R = 15 Å with Q = 0.102 Cm^{-2} in 1 M of 1:2:1 mixed salt ($NaCl/MgCl_2$) solution with different Mg^{2+}/Na^+ ratios as (a) pure NaCl, (b) 1/4, (c) 1/2, and (d) pure $MgCl_2$, keeping the bulk solvent density (ρ_4^{0*}) fixed at 0.4. Symbols and lines represent simulation results and DFT predictions, respectively. Solid symbols and solid lines represent SRPM system; Empty symbols and dashed lines are for the RPM case. The different lines and symbols correspond to green, ○: Cl^-; blue, Δ: solvent molecules; black, □: Na^+; and red, ★: Mg^{2+}, respectively.

sum contribution seems to be negligible for the current system. For efficient sampling, the condition for the acceptance ratio is maintained in the range of 0.2 to 0.4. The final equilibrated density distributions are justified after total moves of 8×10^8 and final density profiles are reported after applying block averaging procedure.

III. RESULTS AND DISCUSSION

In the present work, we carry out a systematic study of the structure of SDL around a spherical macroion formed by the electrolyte containing mixture of mono- and multivalent co-ions incorporating the molecular nature of the solvent as an individual component under SRPM formalism. The singlet density profiles of the small ions and the solvent in SDL for the mixed salt, i.e., 1:2:1 ($NaCl/MgCl_2$) with 1 M 1:1 (NaCl) electrolyte at varying concentration of 2:1 ($MgCl_2$) salt are calculated. For direct comparison, we have also included some of the representative plots from RPM results[24] on the same systems. Figure 1a−d depicts density profiles of co-ions, counterions, and solvent molecules around a spherical colloidal macroion of R = 15 Å for 1 M total salt concentrations keeping the bulk solvent density (ρ_4^{0*}) fixed at 0.4 with Q = 0.102 Cm^{-2} and for various mole fractions of NaCl and $MgCl_2$. As expected, there is a significant accumulation of Cl^- counterions at the surface of the macroion, accompanied by a depletion of both Na^+ and Mg^{2+} co-ions in the same region. This is due to the electrostatic interactions between the macroion and the small ions. Interestingly, addition of small amount of divalent Mg^{2+} co-ions [Figure 1b] to NaCl, increases the accumulation of Na^+ near the macroion surface compared to pure NaCl [Figure 1a]. In comparison to RPM case [Figure 1b], there is a significant increase in the densities of both the counterions, Na^+ and Mg^{2+} as well as the co-ions in presence of solvent (SRPM case). As can be seen from Figure 1c, further addition of Mg^{2+} to

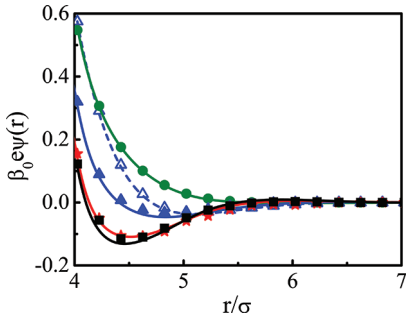

Figure 2. Mean electrostatic potential profiles around a spherical macroion of R = 15 Å with Q = 0.102 Cm^{2-} having 1 M $NaCl/MgCl_2$ solution with different Mg^{2+}/Na^+ ratios as follows: pure NaCl, green, ○; 1:4, blue, Δ; 1:2, red, ★; and pure $MgCl_2$, black, □, keeping the bulk solvent density fixed at (ρ_4^{0*}) = 0.4. Symbols correspond to MC results and lines represent DFT predictions. Solid symbols and solid lines represent the SRPM system; open symbols and dashed lines are for the RPM case.

the bulk solution, at the same Na^+ concentration, results into more accumulation of Na^+ in the vicinity of the macroion. A distinct peak is observed in the density profiles of the ions and solvent at a distance σ away from the macroion surface, where the appearance of charge inversion becomes prominent. This effect is purely attributed to the significance of increased ion−ion correlations and the hard-core exclusion by the macroparticle and small ions. In presence of multivalent co-ions Mg^{2+}, large number of counterions effectively screens the positive charge on the macroion leading to a point where the co-ion density crosses the counterion density, resulting into charge inversion. The damping of the density profiles, as observed in the plots, can also be explained by effective screening of the macroion charge with increasing valence of the co-ion.

The mean electrostatic potential as a function of the distance to the macroion for systems with different Mg^{2+}/Na^+ ratios are plotted in Figure 2. The first thing worth to be noticed is that, the high co-ion valency of the electrolyte resulted in a fast decay of electrostatic potential. The larger number of counterions in presence of higher valent co-ions promotes the screening of surface charge, resulting in a rapid decay of MEP. As can be seen, the value of MEP at the contact of the macroion surface decreases with increasing amount of added divalent co-ions (Mg^{2+}) to the NaCl solution. This observation corroborates the conclusions derived from the density profiles. Further increase of Mg^{2+} keeping Na^+ concentration the same, the sign of MEP profile changes from positive to negative (appearance of the charge inversion point). Subsequently, the MEP profile touches the zero line at a much shorter distance from the surface, indicating the damping of the density profile. However, the MEP profile for the RPM case of the same system always remain higher[24] than the SRPM case indicating that the damping is quite slower in the former case.

To investigate the effect of ion−ion correlation we have considered four different $NaCl/MgCl_2$ mixed electrolyte systems of concentration 0.01 M, 0.1 M, 1 and 2 M, maintaining 2:1 ($MgCl_2$) and 1:1 (NaCl) salt concentration ratio as 1:2 (i.e., Mg^{2+}/Na^+ = 1/2) in each case. For each system, the macroion radius and surface charge density and small ion diameter are kept unchanged as that of Figure 1. Figure 3a−d depicts the variation of normalized density profile with respect to the bulk density [$\rho_\alpha(r)/\rho_\alpha^0$] for both the co-ions, counterions, and solvent molecules as a function of distance from the macroion surface

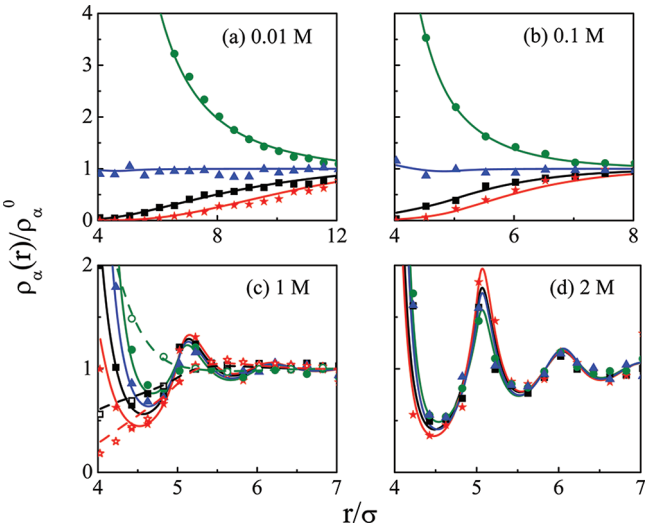

Figure 3. Small ion density profiles around a spherical macroion of $R = 15$ Å with $Q = 0.102$ Cm^{-2} having 1 M NaCl/$MgCl_2$ solution with $Mg^{2+}/Na^+ = 1/2$ at various electrolyte concentrations: (a) 0.01 M, (b) 0.1 M, (c) 1 M, and (d) 2 M. Bulk solvent density (ρ_4^{0*}) is kept constant at (a) 0.004, (b) 0.04, (c) 0.4, and (d) 0.4. The key is the same as in Figure 1.

corresponding to the bulk solvent density (ρ_4^{0*}) as (a) 0.004, (b) 0.04, (c) 0.4, and (d) 0.4 respectively. At lower concentration, the density profile of solvent remains nearly constant, although, there exists accumulation and depletion of counterions and co-ions respectively at the surface of the charged macroparticle. On increasing the electrolyte concentration, the ionic density as well as solvent density increases at the interface. The appearance of oscillations in density profiles of small ions as well as solvent becomes prominent at 1 M [Figure 3c]. The density of solvent being much higher than that of small ions, the hard sphere repulsion between the ions and the solvent become predominant due to efficient packing that leads to preferential accumulation of all components at the surface of the macroion. This packing contribution in addition to the electrostatic interaction will lead to higher accumulation of counterions and an increase in co-ion concentration at the surface. If electrostatic potential were the dominating one in the system, then with increase in electrolyte concentration the co-ion density at the surface would follow the opposite trend as can be seen[24] in RPM case for 1 M system [Figure 3c]. As a result of increase of solvent density alongwith the electrolyte concentration the packing contribution becomes predominant over the electrostatic interaction leading to accumulation of co-ion at the surface of the spherical macroion. Higher accumulation of ions at the surface leads to sharp screening of macroion charge resulting to a narrow diffused layer. At higher electrolyte concentration the double layer becomes more structured. This is reflected as strong oscillation and layering in the density profiles of counterions, co-ions, and solvent molecules for concentrated (1 and 2 M) electrolyte system.

The variation of MEP as a function of distance from the surface of the macroion for systems corresponding to Figure 3 has been shown in Figure 4. From the plot, it is observed that the mean electrostatic potential at the surface decreases with an increase in ionic concentrations. This is due to better screening of surface potential associated with higher accumulation of counterions at the surface at increased concentration of the electrolyte. At lower concentration (0.01 and 0.1 M) the MEP profiles

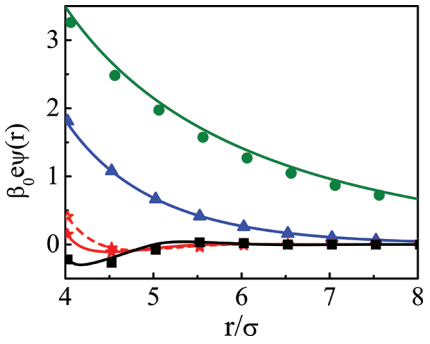

Figure 4. Mean electrostatic potential profiles around a spherical macroion of $R = 15$ Å with $Q = 0.102$ Cm^{-2} having 1 M NaCl/$MgCl_2$ solution with $Mg^{2+}/Na^+ = 1/2$ at various electrolyte concentrations 0.01 M (Green, ○), 0.1 M (Blue, Δ), 1 M (Red, ★), and 2 M (Black, □). Bulk solvent density (ρ_4^{0*}) is kept constant at 0.004 for 0.01 M, 0.04 for 0.1 M, and 0.4 for both 1 and 2 M mixed electrolyte solutions. Symbols are MC results and lines represent DFT predictions. Solid symbols and solid lines represent SRPM system; Empty symbols and dashed lines are for the RPM case.

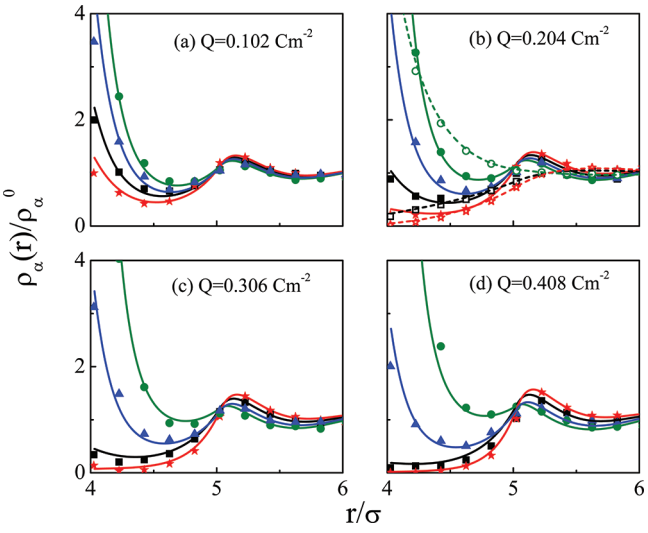

Figure 5. Small ion density profiles for a 1 M NaCl/$MgCl_2$ mixed electrolyte systems with $Mg^{2+}/Na^+ = 1/2$ around a spherical macroion of $R = 15$ Å at various surface charge densities (a) $Q = 0.102$ Cm^{-2}, (b) $Q = 0.204$ Cm^{-2}, (c) $Q = 0.306$ Cm^{-2}, and (d) $Q = 0.408$ Cm^{-2}, keeping bulk solvent density (ρ_4^{0*}) fixed at 0.4. The key is the same as in Figure 1.

decay to zero monotonically. At 1 M concentration, the profile changes sign and passes through a minimum at negative value. As expected, the MEP profile for the RPM system stays higher,[24] although it shows lower charge inversion compared to SRPM case. However, for $c = 2$ M, the MEP profile starts from the negative value and becomes positive. The MEP profile indicates that the potential inversion is predicted to start from 1 M of the mixed electrolyte system under solvent restricted primitive model. The charge inversion as observed in case of density profiles discussed in the previous section results in the potential inversion.

We also investigated the influence of macroion surface charge density on the density distribution of small ions and solvent molecules in the double layer. For this purpose, we have taken

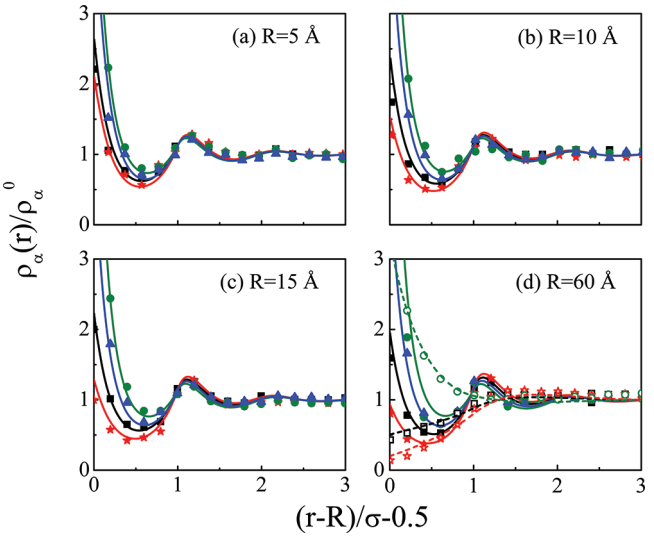

Figure 6. Small ion density profiles for a 1 M $NaCl/MgCl_2$ mixed electrolyte systems with $Mg^{2+}/Na^+ = 1/2$ around a spherical macroion with $Q = 0.102$ Cm^{-2} having radius (a) $R = 5$ Å, (b) $R = 10$ Å, (c) $R = 15$ Å, and (d) $R = 60$ Å, keeping bulk solvent density (ρ_4^{0*}) fixed at 0.4. The key is the same as in Figure 1.

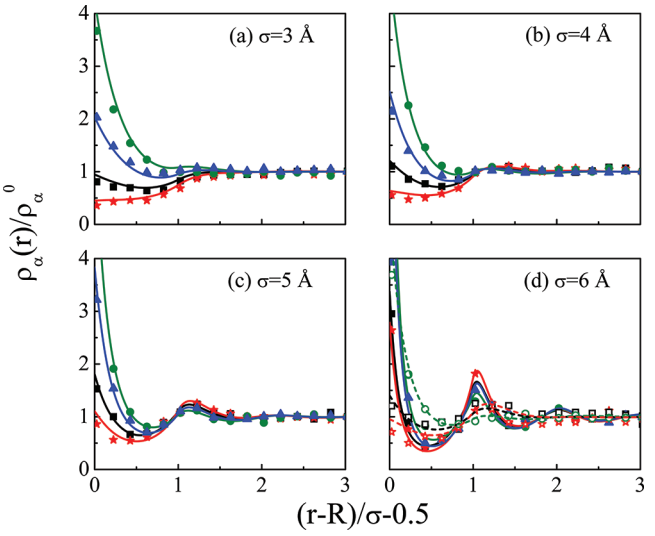

Figure 7. Small ion density profiles around a spherical macroion of $R = 15$ Å with $Q = 0.102$ Cm^{-2} in 1 M $NaCl/MgCl_2$ mixed electrolyte systems with $Mg^{2+}/Na^+ = 1/2$ at different small ion diameter of (a) 3, (b) 4, (c) 5, and (d) 6 Å, keeping bulk solvent density (ρ_4^{0*}) fixed at 0.25. The key is the same as in Figure 1.

four systems of $NaCl/MgCl_2$ mixed electrolyte keeping Mg^{2+}/Na^+ as 1/2 at $c = 1$ M with varying surface charge densities for the macroion ($R = 15$ Å), where bulk solvent density is fixed at 0.4. Figure 5a–d depicts the density profiles of counterions, co-ions, and solvent molecules at four different surface charge densities, viz., 0.102, 0.204, 0.306, and 0.408 Cm^{-2}, respectively. The accumulation of Cl^- increases at the surface while the depletion of both Na^+ and Mg^{2+} enhances as the surface charge density increases. The depleted co-ions (Na^+ and Mg^{2+}) from the first layer get accumulated in the second layer leading to stronger charge inversions. Due to stronger electrostatic interactions, charge inversion becomes more prominent as the surface charge density increases. Even though the ionic densities are quite lower in the RPM case, it still predicts[24] charge inversion with increase in surface charge density. Interestingly, irrespective of the surface charge density of the macroion, the density profiles merge together after the second layer of accumulation, indicating that the diffused layer width is independent of the macroion surface charge density. This phenomenon can be explained by the hard sphere exclusion effects associated with fixed number of hard spheres as components in all the systems presented here. The predictions from DFT and Monte Carlo simulation study quantitatively agree with each other.

The effect of macroion size on the ionic and solvent density on the $NaCl/MgCl_2$ mixed electrolyte system (1 M) with Mg^{2+}/Na^+ ratio as 1/2, has been shown in the Figure 6a–d. Four different macroion radii, viz., $R = 5$, 10, 15, and 60 Å have been taken into account, while keeping fixed values of the surface charge density (Q) as 0.102 Cm^{-2}, the bulk solvent density at 0.4, and the small ion diameter at 4.25 Å. There occurs significant accumulation of the counterion and depletion of both the co-ions at the interface with the increase of macroion size. This is due to the substantial increase of value of absolute charge (Ze) on the macroion with the increase of macroion radius at a constant surface charge density. At the increased macroion radii, the charge is screened so effectively that the density profile of both the co-ions crosses that of the counterion indicating the appearance of

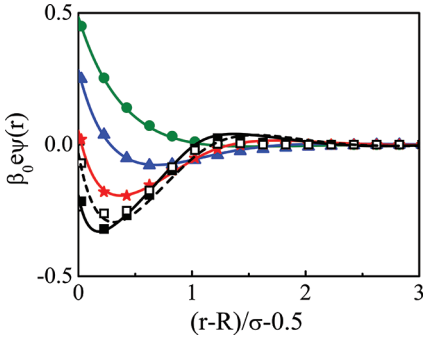

Figure 8. Mean electrostatic potential profiles around a spherical macroion of $R = 15$ Å with $Q = 0.102$ Cm^{-2} in 1 M $NaCl/MgCl_2$ mixed electrolyte systems with $Mg^{2+}/Na^+ = 1/2$ at different small ion diameter of 3 Å (green, ○), 4 Å (blue, Δ), 5 Å (red, ★), and 6 Å (black, □), keeping bulk solvent density (ρ_4^{0*}) fixed at 0.25. Symbols are MC results and lines represent DFT predictions. Solid symbols and solid lines represent SRPM system; Empty symbols and dashed lines are for the RPM case.

phenomena of charge inversion. The same inference also hold good in the RPM case.[24] It can be seen that the density profiles of all the components merge just after the first maxima for lower macroion radius while they are distinctly separated at the increased macroion size.

We also study the effect of variation of ionic size on the density profile and MEP for 1 M $NaCl/MgCl_2$ electrolyte with the Mg^{2+}/Na^+ as 1/2. Figure 7a–d depicts the ionic as well as solvent concentration profile in the vicinity of the macroion ($R = 15$ Å) surface for small ion diameter (σ) 3, 4, 5, and 6 Å, respectively, at the bulk solvent density of 0.25 in each case at a fixed surface charge density of 0.102 Cm^{2-}. As the ionic size increases, the value of the normalized density of counterions, co-ions, and solvent molecules at the macroion surface increases. The oscillation in density profiles also increases as the ionic diameter increases.

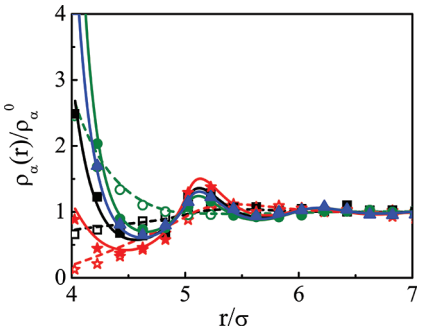

Figure 9. Small ion density profiles for 1 M $NaCl/AlCl_3$ electrolyte with $Al^{3+}/Na^+ = 1/2$, around a spherical macroion of $R = 15$ Å and $Q = 0.102$ Cm^{-2}, keeping bulk solvent density (ρ_4^{0*}) fixed at 0.25. Symbols are simulation results and lines correspond to DFT predictions. Solid symbols and solid lines represent SRPM system; Empty symbols and dashed lines are for the RPM case. The different lines and symbols correspond to green, ○: Cl^-; blue, Δ: solvent molecules; black, □: Na^+; and red, ★: Mg^{2+}, respectively.

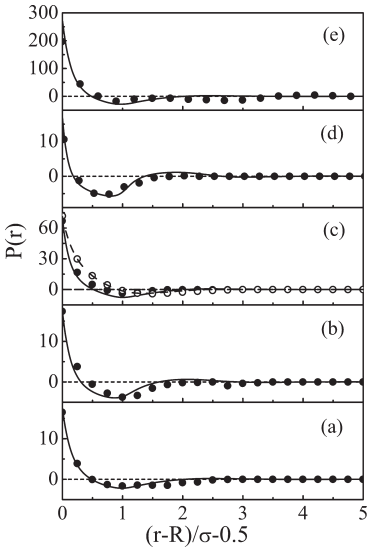

Figure 10. Integrated charge distribution function profiles for 1 M mixed salt with a bulk solvent solvent around a spherical macroion under different parametrical conditions: (a) $NaCl/MgCl_2$ salt, $Mg^{2+}/Na^+ = 1/2$, $R = 15$ Å, $Q = 0.102$ Cm^{-2}, $\sigma = 4.25$ Å, $\rho_4^{0*} = 0.4$; (b) same as (a), except $NaCl/AlCl_3$ salt, $Al^{3+}/Na^+ = 1/2$, $\rho_4^{0*} = 0.25$; (c) same as (a), except $\sigma = 4.25$ Å, $\rho_4^{0*} = 0.25$; (d) same as (a), except $Q = 0.408$ Cm^{-2}; (e) same as (a), except $R = 60$ Å. Symbols are simulation results and lines correspond to DFT predictions. Solid symbols and solid lines represent SRPM system; Empty symbols and dashed lines are for the RPM case.

In case of $\sigma = 3$ Å [Figure 7a], all the density profiles merge to the bulk density accompanied by the usual decay of counterions and solvent molecules and the growth of the co-ions. At $\sigma = 4$ Å [Figure 7b], before merging to the bulk density profile, they all form a layer, where the both the co-ion density crosses the counterion density. This is because of charge inversion, which arises due to efficient shielding of the macroion surface charge. The phenomena become more prominent as the size of small ions increases further ($\sigma = 5, 6$ Å) [Figure 7, panels c and d] and appears at shorter distance from the macroion surface. The density profiles also form more number of layers before saturating to the bulk density. The MEP profile (Figure 8) also corroborates the same conclusion as obtained from the density profile. At $\sigma = 3$ Å, the MEP profile decays to zero monotonically, while the profile changes sign and passes through a minimum at negative value for $\sigma = 4, 5$, and 6 Å. As a consequence of increasing the ionic size, the effect of exclusion volume becomes significant to push the small ions near to the macroion surface. Subsequently, the ionic as well as the solvent molecules get more populated in the vicinity of the macroion surface at larger ionic size.

The effect of the trivalent co-ion (Al^{3+}) on the behavior of double layer characteristics have been studied with the mixed electrolyte $NaCl/AlCl_3$ with Al^{3+}/Na^+ ratio as 1/2 and bulk concentration of 1:1 salt (NaCl) is 1 M. For this purpose, we have taken the system with macroion radius of $R = 15$ Å and small ion diameter as $\sigma = 4.25$ Å at the bulk solvent density of 0.4 and at a surface charge density of 0.102 Cm^{-2}. Figure 9 presents the density profiles of all the components as a function of distance from the macroion surface. The first point to be noted is that the normalized density value of Al^{3+} at the macroion surface is lower compared to that of Mg^{2+} [cf. Figure 1c] in the $NaCl/MgCl_2$ system. This is solely due to stronger electrostatic repulsion between the macroion and the trivalent co-ion (Al^{3+}) compared to the divalent co-ion (Mg^{2+}). Interestingly, the height of the second layer peak is higher in case of 1:3:1 system compared to 1:2:1 system. The co-ion density crosses that of the counterion at a shorter distance from the macroion surface; that is, charge inversion is more prominent in the presence of trivalent co-ion compared to the divalent co-ion. The number of counterion present in the 1:3:1 system is higher compared to that in the 1:2:1 system. Consequently, the macroion charge is screened more effectively in presence of trivalent co-ion. Charge inversion is also visible in the RPM case,[24] although the overall ionic densities are substantially lower than the MSM profiles.

A better interpretation of the behavior of the SDL in terms of charge compensation and layering can be interpreted in terms of integrated charge distribution function $P(r)$ defined as

$$P(r) = Z + \int_0^r d\mathbf{r}' \sum_\alpha z_\alpha \rho_\alpha(\mathbf{r}') \qquad (12)$$

which represents the net charge within a sphere of radius r. Figure 10 depicts the integrated charge profiles for the SDL over a wide range of parametric conditions. Each profile decays to a minimum starting from a positive value and reaches to the zero level at the bulk limit to maintain the electroneutrality condition. There appears clear charge inversion in presence of multivalent co-ions [Figure 10a for Mg^{2+} and 10b for Al^{3+}] due to the combined effect of stronger electrostatic interaction and larger counterion concentration. Increase of macroion surface charge density also enhances the charge inversion [Figure 10c] by amplifying the charge correlation. The magnitude of charge inversion is lower and the decay of the integrated charge profile is slower for the RPM case.[24] Larger excluded volume effect due to increase of ionic diameter ($\sigma = 6$ Å) pushes the small ions toward the macroion surface resulting the appearance of charge inversion at a much shorter distance [Figure 10d]. However, increase in the macroion size ($R = 60$ Å) causes the charge and size correlations to play simultaneously on the behavior of SDL [Figure 10e].

IV. CONCLUDING REMARKS

In the present study, a systematic investigation of the structure of colloidal solution in presence of $NaCl/MgCl_2$ mixed electrolyte system, which resembles the spherical electric double layers, is performed in detail by using the MC simulations and density

functional approach, where the solvent molecule is considered as fourth component. Here, the colloid particle is mimicked by a hard sphere having uniform surface charge density immersed in a uniform dielectric continuum surrounded by the small ions (all of equal diameter) and solvent molecules, that are represented by charged and neutral hard spheres, respectively. The model is quite realistic and shows much richer double layer characteristics than the restrictive primitive model due to the incorporation of the molecular nature of the solvent component. Standard canonical MC simulation is performed to get the equilibrium ionic as well as solvent density profile in the vicinity of macroion and the mean electrostatic potential in the system. The density functional approach is partially perturbative where hard sphere contribution to the free energy is calculated through weighted density approximations (WDA) and the residual Coulombic contribution is treated perturbatively with bulk second order correlation function taken from mean spherical approximation. The system is studied over a wide range of parametric conditions, such as at different ionic valences as well as size, at varying electrolyte concentrations ratio of mono- and multivalent co-ions of mixed electrolytes, at different surface charge densities and radius of the macroion. The theoretical predictions in terms of the density profiles of all the components and the mean electrostatic potential profiles are found to be in good agreement with the Monte Carlo simulation results. The oscillations in density profiles, the layering and the charge inversion phenomena are indications of hard sphere exclusion effects, those are synergised directly due to consideration of the molecular nature of the solvent.

With increase in electrolyte concentration, the layering and oscillations in density profiles increased quite significantly due to volume exclusion. Thus, increase in concentration leads to shortening of diffuse layer width. The steric interactions due to the presence of solvent molecules in excess causes the charge inversion in the density profiles of 2 M mixed electrolyte solution. Again on increasing the valence of the co-ion, the oscillations and layering of the density profile increase. More is the surface charge density on the surface of the macroion, higher is the accumulation of counterions and depletion of co-ions at the surface due to stronger electrostatic correlations. The mean electrostatic potential profiles merely corroborates the findings brought from the density profiles. In general, the magnitude of the MEP is lower in SRPM compared to RPM due to both size and charge correlations. In almost all the cases DFT and MC simulations go hand in hand.

Although this simplistic model is quite successful in explaining the two important phenomena, viz. layering and charge inversion, related to electrical double layer, it still remains to be primitive. It will be of interest to include a minimum level of complexity like the dipolar or quadrupolar nature of the solvent and observe its effect on the diffuse layer. How the zeta potentials as well as the interfacial capacitances vary on changing different parameters including the solvent, will be another important area of study. The general effect of charge as well as the size asymmetry on the structure of SDL through the use of MSA correlation functions is currently under progress and will be reported in days to come.

AUTHOR INFORMATION

Corresponding Author

*E-mail: chandra@barc.gov.in.

Notes

[†]Also at Homi Bhabha National Institute (HBNI), Mumbai, India.

ACKNOWLEDGMENT

The authors thank Tulsi Mukherjee for his kind interest and constant encouragement. The authors gratefully acknowledge support from the INDO-EU project MONAMI on Computational Materials Science.

REFERENCES

(1) Carnie, S. L.; Torrie, G. M. *Adv. Chem. Phys.* **1984**, *56*, 141.
(2) Hansen, J. P.; Löwen, H. *Annu. Rev. Phys. Chem.* **2000**, *51*, 209.
(3) *Interfacial Processes and Molecular Aggregation of Surfactants*; Narayanan, R., Ed.; Springer: Berlin, 2008.
(4) Evans, D. F.; Wennerström, H. *The Colloidal Domain: Where Physics, Chemistry, Biology and Technology Meet*; Wiley-VCH: New York, 1994.
(5) Hunter, R. J. *Foundations of Colloid Science*; Oxford University Press: New York, 1985.
(6) Durand-Vidal, S.; Simonin, J. P.; Turq, P. *Electrolytes at Interfaces*; Kluwer Academic: Dordrecht, 2000.
(7) Borkovec, M.; Behrens, S. H.; Semmler, M. *Langmuir* **2000**, *16*, 5209.
(8) Zhou, H.-X.; Rivas, G.; Minton, A. P. *Annu. Rev. Biophys.* **2008**, *37*, 375.
(9) Lozada-Cassou, M. In *Fundamentals of Inhomogeneous Fluids*; Henderson, D., Ed.; Marcel Dekker: New York, 1992.
(10) Torrie, G. M.; Valleau, J. P. *J. Phys. Chem.* **1982**, *86*, 3251.
(11) Lozada-Cassou, M.; Saavedra-Barrera, R.; Henderson, D. *J. Chem. Phys.* **1982**, *77*, 5150.
(12) Crozier, P. S.; Rowley, R. L.; Henderson, D. *J. Chem. Phys.* **2001**, *114*, 7513.
(13) Boda, D.; Fawcett, W. R.; Henderson, D.; Sokolowski, S. *J. Chem. Phys.* **2002**, *116*, 7170.
(14) Gonzales-Tovar, E.; Lozada-Cassou, M.; Henderson, D. *J. Chem. Phys.* **1985**, *83*, 361.
(15) Hribar, B.; Vlachy, V.; Bhuiyan, L. B.; Outhwaite, C. W. *J. Phys. Chem. B* **2000**, *104*, 11522.
(16) Deserno, M.; Jiménez-Ángeles, F.; Holm, C.; Lozada-Cassou, M. *J. Phys. Chem. B* **2001**, *105*, 10983.
(17) Patra, C. N.; Chang, R.; Yethiraj, A. *J. Phys. Chem. B* **2004**, *108*, 9126.
(18) Goel, T.; Patra, C. N.; Ghosh, S. K.; Mukherjee, T. *J. Chem. Phys.* **2010**, *132*, 194706.
(19) González-Tovar, E.; Lozada-Cassou, M. *J. Chem. Phys.* **1989**, *93*, 3761.
(20) Degréve, L.; Lozada-Cassou, M.; Sánchez, E.; González-Tovar, E. *J. Chem. Phys.* **1993**, *98*, 8905.
(21) Yu, Y. X.; Wu, J. Z.; Gao, G. H. *J. Chem. Phys.* **2004**, *120*, 7223.
(22) Guerrero-García, G. I.; González-Tovar, E.; Lozada-Cassou, M.; Guevara-Rodríguez, F.; de, J. *J. Chem. Phys.* **2005**, *123*, 034703.
(23) Goel, T.; Patra, C. N. *J. Chem. Phys.* **2007**, *127*, 034502.
(24) Patra, C. N. *J. Phys. Chem. B* **2010**, *114*, 10550.
(25) Rickayzen, G. *J. Chem. Phys.* **1999**, *111*, 1109.
(26) Bulavchenko, A. I.; Batishchev, A. F.; Batishcheva, E. K.; Torgov, V. G. *J. Phys. Chem. B* **2002**, *106*, 6381.
(27) Patra, C. N. *J. Phys. Chem. B* **2009**, *113*, 13980.
(28) Schmitz, K. S. *Macroions in Solution and Colloidal Suspension*; VCH: New York, 1993.
(29) Israelachvili, J. *Intermolecular and surface forces*; Academic Press: London, 1992.
(30) Safran, S. A. *Statistical Thermodynamics of Surfaces, Interfaces, and Membranes*; Addison-Wesley: Reading, MA, 1994.
(31) Hara, M. *Polyelectrolytes: Science and Technology*; Marcel Dekker: New York, 1993.
(32) Smagala, T. G.; Patrykiejew, A.; Pizio, O.; Fawcett, W. R.; Sokolowski, S. *J. Chem. Phys.* **2008**, *128*, 024907.
(33) Bhuiyan, L. B.; Vlachy, V.; Outhwaite, C. W. *Int. Rev. Phys. Chem.* **2002**, *21*, 1.

(34) Jiménez-Ángeles, F.; Lozada-Cassou, M. *J. Phys. Chem. B* **2004**, *108*, 7286.
(35) Gelbart, M. W.; Bruinsma, R. F.; Pincus, P. A.; Parsegian, V. A. *Phys. Today* **2000**, *53*, 38.
(36) Tang, Z.; Scriven, L. E.; Davis, H. T. *J. Chem. Phys.* **1992**, *97*, 494.
(37) Lamperski, S.; Pluciennik, M. *Mol. Simul.* **2010**, *36*, 111.
(38) Mittal, J.; Best, R. B. *Proc. Natl. Acad. Sci. U.S.A.* **2008**, *105*, 20233.
(39) Hiemenz, P. C.; Rajagopalan, R. *Principles of Colloid and Surface Chemistry*; Marcel Dekker: New York, 1997.
(40) Bhuiyan, L. B.; Outhwaite, C. W. *Condens. Matter Phys.* **2005**, *8*, 287.
(41) Evans, R. In *Fundamentals of Inhomogeneous Fluids*; Henderson, D., Ed.; Marcel Dekker: New York, 1992.
(42) Denton, A. R.; Ashcroft, N. W. *Phys. Rev. A* **1991**, *44*, 8242.
(43) Waisman, E.; Lebowitz, J. L. *J. Chem. Phys.* **1972**, *56*, 3086.
(44) Metropolis, N.; Rosenbluth, A. W.; Rosenbluth, M. N.; Teller, A. H.; Teller, E. *J. Chem. Phys.* **1953**, *21*, 1087.